Antisense Binding Enhanced by Tertiary Interactions: Binding of Phosphorothioate and N3′→P5′ Phosphoramidate Hexanucleotides to the Catalytic Core of a Group I Ribozyme from the Mammalian Pathogen *Pneumocystis carinii*†

Stephen M. Testa,‡ Sergei M. Gryaznov,§ and Douglas H. Turner*,‡

Department of Chemistry, University of Rochester, Rochester, New York 14627-0216, and Geron Corporation, 230 Constitution Drive, Menlo Park, California 94025

Received January 12, 1998; Revised Manuscript Received May 4, 1998

ABSTRACT: *Pneumocystis carinii* is the most common lethal opportunistic pathogen infecting Acquired Immune Deficiency Syndrome (AIDS) patients, and more effective therapeutics for it are needed. *P. carinii*, but not humans, contain RNA self-splicing group I introns, so these functionally important RNAs are potential anti-fungal targets. *In vitro,* d(ATGACT), which mimics the 3′ end of the 5′ exon of a conserved ribosomal RNA group I intron from mouse-derived *Pneumocystis carinii* binds to a ribozyme that is a truncated form of this intron. The binding is about 30,000 times tighter than expected for simple base-pairing because binding is enhanced by tertiary interactions. Here we report the effects of modifying the phosphodiester backbone of d(ATGACT) with phosphorothioate and of d(ATGAC)rU with N3′→P5′ phosphoramidate linkages. The enhancement of binding by tertiary interactions is not substantially decreased, and in some cases is increased when single R_p and S_p phosphorothioate substitutions are made, although overall binding is weaker by up to 6-fold. A mixture of 5′ exon mimic isomers that each contain five phosphorothioate linkages binds to the ribozyme at least 14-fold less tightly than the corresponding phosphodiester mimic. In contrast, the 5′ exon mimic with five internal N3′→P5′ phosphoramidate linkages binds 4-fold more tightly than d(ATGAC)rU. This increased binding is largely due to more favorable base-pairing, but tertiary interactions still enhance binding by more than 2,000-fold. These results indicate that chemically modified, nuclease stable 5′ exon mimics can act as antisense agents with binding enhanced by tertiary interactions (BETI). This strategy permits design of short antisense agents with high specificity.

Some fungal opportunistic pathogens have RNA elements that can serve as molecular targets for pharmacological intervention. Group I introns are one example (*1, 2, 3*). A potential strategy for targeting RNA is to use antisense oligonucleotides that base-pair to the target (*4, 5*). Binding stability and specificity can be enhanced, however, if short antisense agents can also exploit stabilizing tertiary interactions (Figure 1) (*6, 7*). We have previously shown that ribo and deoxyribonucleotide hexamers can exploit stabilizing tertiary interactions of a ribosomal RNA group I ribozyme from the mouse-derived opportunistic fungal pathogen *Pneumocystis carinii* to bind more than 30,000 times tighter than measured for base-pairing (*7*). Ribo and deoxyribonucleotides, however, are rapidly degraded by cellular nucleases *in vivo* (*8, 9*). Therefore, to serve as therapeutics, antisense oligonucleotides must be protected from cellular nucleases. This is usually done by chemically modifying the oligonucleotide backbone (reviewed in *10*−*14*). Potentially useful modifications include phosphorothioate (*15*−*17*) and N3′→P5′ phosphoramidate linkages (*18*−*20*) as replacements for the normal phosphodiester backbone (Figure 2). In this report, we show that DNA hexamers containing nuclease-stable phosphorothioate and N3′→P5′ phosphoramidate backbones can also bind to the *P. carinii* group I ribozyme, P-8/4x, with tertiary stabilization. With d(ATGACT), substituting one phosphodiester per mimic with a phosphorothioate linkage does not substantially reduce, and in some cases enhances tertiary stabilization, although overall binding is weaker by up to 6-fold. Substituting every internal phosphodiester with a phosphorothioate linkage makes overall binding weaker by at least 14-fold. Substituting every internal phosphodiester of d(ATGAC)rU with a phosphoramidate linkage reduces tertiary stability 30-fold. Because of differences in base-pairing stability, however, the phosphoramidate mimic binds to the ribozyme about 4-fold more tightly than the all phosphodiester d(ATGAC)rU. These results show that the phosphodiester backbone of the 5′ exon mimic of the *P. carinii* group I intron can be chemically modified for protection of the oligonucleotide against nuclease degradation while retaining tertiary interactions that dock the 5′ exon mimic into the catalytic core. Implications for ribozyme structure and antisense design are discussed.

MATERIALS AND METHODS

Synthesis and Purification of Nucleic Acids. Unmodified oligonucleotides were synthesized, purified, and 5′ end labeled with [γ-^{32}P]ATP as described (*7*). Phosphorothioate-containing oligodeoxyribonucleotides were synthesized on

† This work was supported by NIH Grant GM22939 to D.H.T. and NIH Postdoctoral Fellowship GM17985 to S.M.T.

* To whom correspondence should be addressed.

‡ University of Rochester.

§ Geron Corp.

S0006-2960(98)00092-0 CCC: $15.00
Published on Web 06/11/1998

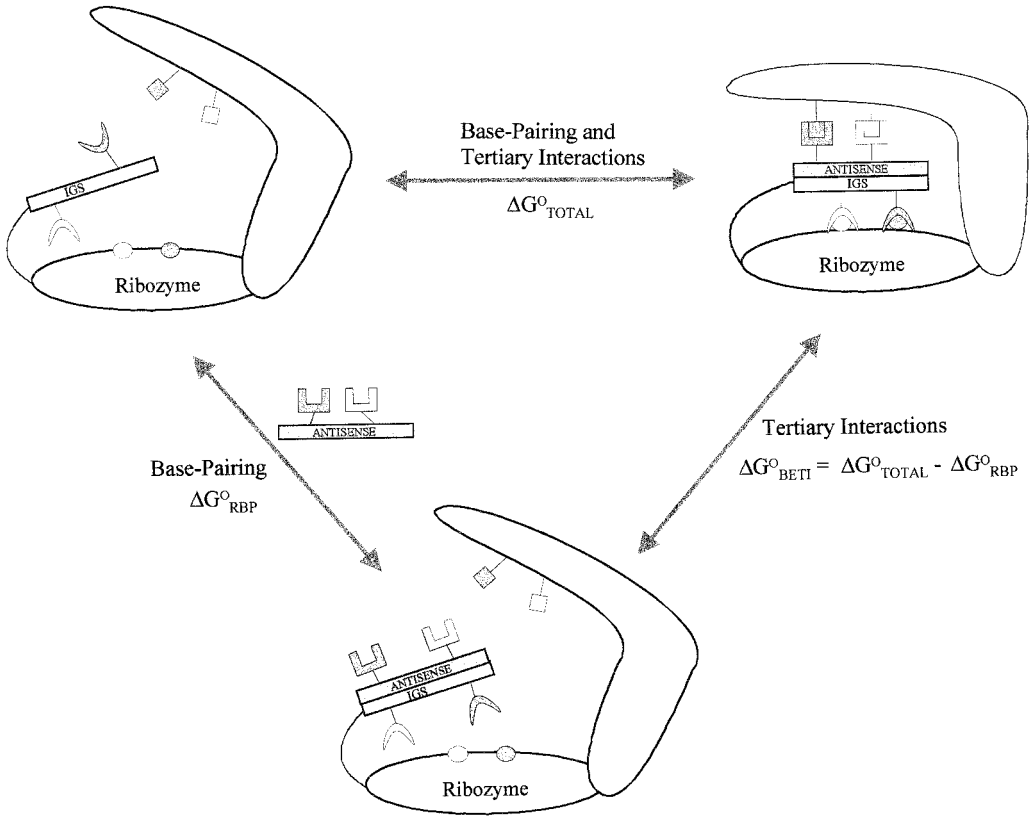

FIGURE 1: A diagrammatic representation of binding enhancement by tertiary interactions (BETI). The ribozyme is initially in an open complex that permits base-pairing of the antisense to the internal guide sequence, IGS, target. Upon forming this helix, certain functional groups are oriented to allow stabilizing tertiary interactions to form between the helix and the ribozyme. For the group I intron of *P. carinii*, the IGS sequence is GGUCAU and the antisense sequence is any hexanucleotide 5′ exon mimic. For the *P. carinii* group I ribozyme, the free energy of tertiary interactions can be more favorable than the free energy derived from base-pair formation (*7*). Since these tertiary interactions depend on the three-dimensional folding of more than 100 nucleotides in the ribozyme (*45*), the result is high specificity in binding.

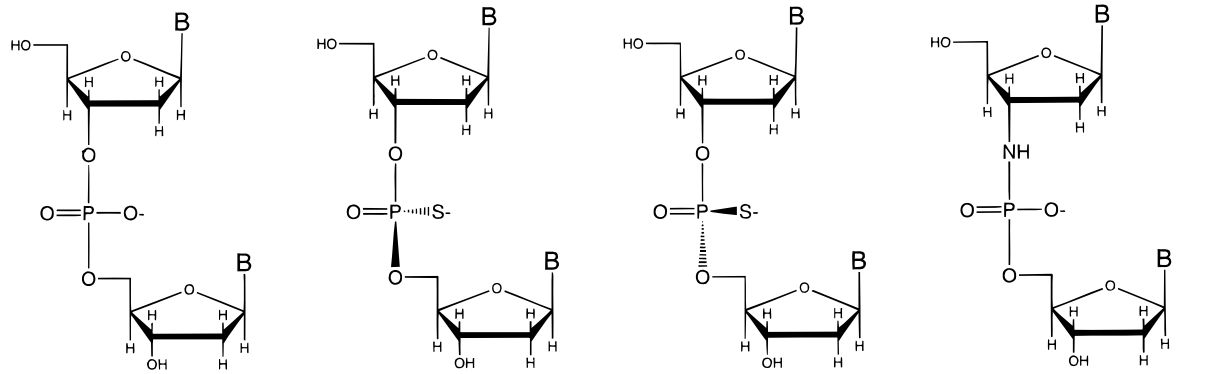

FIGURE 2: The nucleotide backbones used in this study.

an Applied Biosystem RNA/DNA synthesizer using the manufacturer's suggested protocol for trityl-on DNA synthesis. At selected phosphodiester linkages, nonbridging oxygen to sulfur substitutions were generated with Beaucage's reagent (*21*) according to the manufacturers' recommendations (Glen Research, Applied Biosystems). The isomeric mixtures of oligodeoxyribonucleotides were deprotected in concentrated ammonium hydroxide at 55 °C for 4 h and then 12 h at room temperature and purified on Poly-Pak II reverse-phase cartridges (Glen Research) using the manufacturer's protocol, except that 25% acetonitrile was used for the final oligonucleotide elution instead of 15%. The R_p and S_p isomers of each singly substituted oligonucleotide were separated and purified by reverse-phase HPLC (*22*) on a Supelcosil ABZ+ Plus semiprep column (Supelco). The HPLC buffer was 100 mM triethylamine acetate (pH 7.0), the mobile phase was acetonitrile, and the gradient was 0 to17.5% acetonitrile over 1 h at a flow rate of 1 mL/min. The R_p and S_p isomers were assigned based on preferential degradation of the S_p linkage by P1 nuclease (*23*). Except for d(ATG*t*ACT), the R_p isomer had a shorter retention time than the S_p isomer on the reverse phase HPLC column. The observed relative retention times are expected based on previous studies (*22*). All molecules were at least 95% pure.

The concentration of each phosphodiester and phosphorothioate oligonucleotide was estimated from published extinction coefficients for phosphodiester-containing oligonucleotides (*24*).

The phosphoramidate oligonucleotide with a 3′ terminal ribose, d(AnTnGnAnCn)rU, was synthesized, purified, and quantified as previously described (*19*). The molecular weight of d(AnTnGnAnCn)rU was confirmed by electrospray mass spectroscopy on a Hewlett-Packard Series 1100 LC/MSD Chemstation.

The P-8/4x ribozyme was synthesized by T7 RNA polymerase runoff transcription of *Xba* I linearized P-8/4x plasmid and purified as described (*7*). The ribozyme was reannealed to produce the functional structure by incubating at 55 °C in the appropriate buffer for 8 min and then slow cooling to 37 °C.

Determination of K_d for 5′ Exon Mimic Binding to P-8/4x. The dissociation constant, K_d, of each 5′ exon mimic binding to the P-8/4x ribozyme was determined via competition with radiolabeled oligoribonucleotide, r(AUGACU), for binding to the ribozyme at 37 °C via competitive band-shift gel electrophoresis essentially as described (*7*) except the ribozyme was reannealed in 1X rather than 1.5X buffer. The gel and electrophoresis buffers were made from either H15Mg [50 mM Hepes (25 mM Na^+), 15 mM $MgCl_2$, and 135 mM KCl at pH 7.5] or H12Mg3Mn [50 mM Hepes (25 mM Na^+), 12 mM $MgCl_2$, 3 mM $MnCl_2$, and 135 mM KCl at pH 7.5] buffer. Each reported K_d value is the average of at least 3 independent measurements for the phosphorothioates in H15Mg buffer, 2 independent measurements for the phosphoramidate in H15Mg buffer, and a single measurement for the 5′ exon mimics in H12Mg3Mn buffer.

The dissociation constants of the single R_p and S_p phosphorothioate hexamers, d(A*r*TGACT) and d(A*s*TGACT), respectively, binding to the P-8/4x ribozyme in H15Mg buffer at 37 °C were also analyzed by a direct band-shift assay essentially as described (*7*). The relatively weak binding of the all-phosphorothioate d(A*t*T*t*G*t*A*t*C*t*T) to P-8/4x precluded analyzing its binding to the ribozyme by this method.

Optical Melting Curves. The thermodynamics of base-pairing of each 5′ exon mimic with r(GGUCAU), a mimic of the P-8/4x ribozyme's internal guide sequence, was analyzed through thermal denaturation experiments at 280 nm on a Gilford-250 UV−Vis spectrophotometer equipped with a Gilford-2527 thermoprogrammer. The temperature was increased at a rate of 1 °C per min, typically from 0 to 60 °C. The oligonucleotide strand concentration was typically 700 μM. Such high concentrations were required because of the inherently low melting temperatures of the phosphorothioate-containing duplexes. The resultant curves were fit to a two-state nonself-complementary model to quantify the thermodynamic parameters of each duplex (*25*, *26*). The thermodynamic values reported are the averages of at least two independent measurements. For helixes containing the phosphoramidates or the all-phosphorothioate hexamer, d(A*t*T*t*G*t*A*t*C*t*T), in H15Mg buffer, thermodynamic parameters were also extracted from plots of T_m^{-1} vs log(C_T/4), where T_m is the melting temperature in Kelvins and C_T is the total oligonucleotide concentration (*27*). Six concentrations were analyzed over an 80-fold range (9−720 μM). The agreement of the enthalpy change to within 16% between the two methods suggests the system is close to two-state. The all-phosphorothioate hexamer, however, is a mixture of 32 stereoisomers so that it is not a two-state system. Thus the thermodynamic values are approximate. The low stability of the helixes that contain a single phosphorothioate precludes analyzing the concentration dependence of their melting temperatures. Therefore, the reported values for these helixes are also approximations. Since the internal guide sequence mimic, r(GGUCAU), exhibits self-complementary duplex formation in the same temperature range (*7*, *25*), the reported hybrid duplex stabilities are considered upper limits.

RESULTS

Binding of 5′ Exon Mimics to the P-8/4x Ribozyme. Dissociation constants for 5′ exon mimics binding to the P-8/4x ribozyme were measured by competitive band-shift native gel electrophoresis (Figure 3). The results are listed in Table 1. The dissociation constants of d(A*r*TGACT) and d(A*s*TGACT) were also measured by a direct band-shift assay (Table 1). Each single phosphorothioate substitution increases the K_d relative to d(ATGACT) by between 2 and 6-fold. The S_p isomer is more destabilizing than the R_p isomer at every phosphorothioate linkage except for position −3, as defined in Figure 4.

Competitive band-shift electrophoresis binding assays were also conducted with 3 mM Mn^{2+} in a background of 12 mM Mg^{2+}, and compared to results in 15 mM Mg^{2+}. Since Mn^{2+} coordinates more strongly to sulfur than Mg^{2+}, any reduction in stability due to the loss of Mg^{2+}-oxygen contacts for the phosphorothioates can be at least partially recovered by adding Mn^{2+} (*28*−*30*). The inclusion of Mn^{2+} results in more than a 10-fold increase in binding of the *all phosphodiester* 5′ exon mimic, d(ATGACT), to the P-8/4x ribozyme. In comparison, the stability increase is about 20-fold for the singly substituted mimic, d(ATG*r*ACT), and at least 20-fold for the all-phosphorothioate, d(A*t*T*t*G*t*A*t*C*t*T).

As shown in Table 1, the 5′ exon mimic that contains an internal phosphoramidate backbone, d(AnTnGnAnCn)rU, binds to the P-8/4x ribozyme almost 4-fold more tightly than the corresponding all phosphodiester mimic d(ATGAC)rU.

Binding of 5′ Exon Mimics to the Oligonucleotide, r(GGUCAU). The stability of base-pairing between 5′ exon mimics and the P-8/4x ribozyme was estimated from the stability of duplex formation of each mimic with the oligonucleotide, r(GGUCAU), which has the sequence of the base-pairing region of the internal guide sequence of the ribozyme (Figure 4). The stability of each duplex was estimated by UV thermal melting in either H15Mg or H12Mg3Mn buffer (Tables 1 and 2).

The single phosphorothioate containing duplexes in H15Mg show a decrease of 0.5 to 1.5 kcal/mol in stability relative to the d(ATGACT) • r(GGUCAU) duplex. Based on studies of a DNA 14-mer with AT base-pairs, the all-phosphorothioate is expected to be less stable than partially substituted duplexes (*31*). Surprisingly, the isomeric mixture of completely substituted 5′ exon mimics appears to form the most stable duplex with r(GGUCAU). It is likely that the stability of the all-phosphorothioate duplex, however, is overestimated because of the presence of a significant fraction of r(GGUCAU) homoduplex (*7*), which forms because the multiple

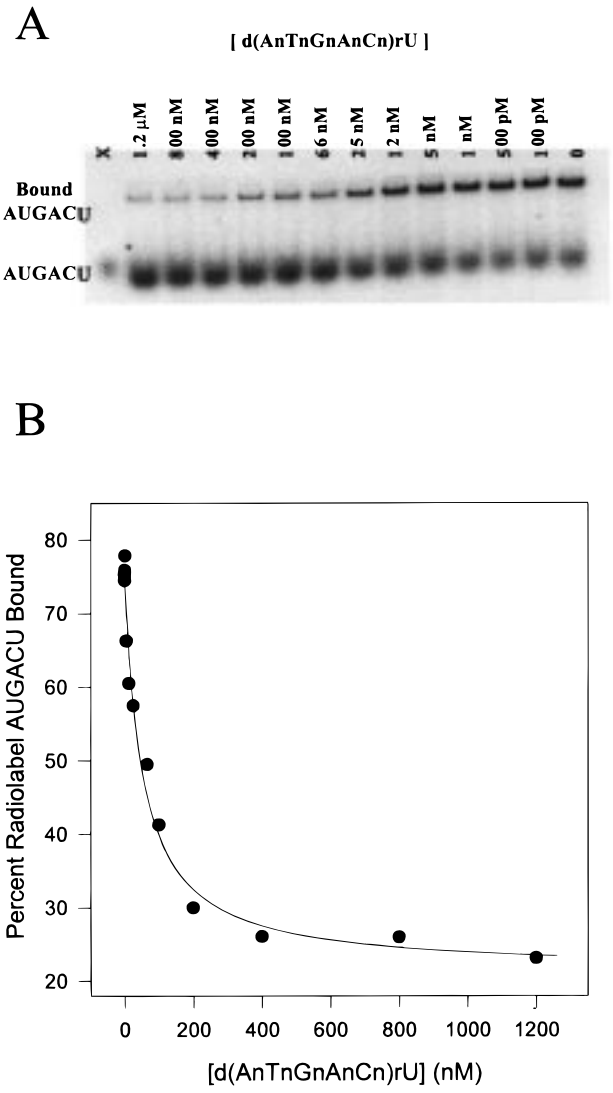

FIGURE 3: A typical competition band-shift assay run on a native polyacrylamide gel. The phosphoramidate 5′ exon mimic d(AnTnGnAnCn)rU competes with the unmodified, radiolabeled 5′ exon mimic, r(AUGACU), for binding to the P-8/4x ribozyme in 50 mM Hepes (25 mM Na^+), 15 mM $MgCl_2$, and 135 mM KCl at pH 7.5. (A) The partitioning of bound and free radiolabeled r(AUGACU) as a function of the concentration (listed above each corresponding lane) of added competitor, d(AnTnGnAnCn)rU. Lane X contains only free radiolabeled r(AUGACU). (B) The plot and fitted curve of the competition band-shift assay in A.

thioate substituted heteroduplex is relatively unstable. Furthermore, all results with isomeric mixtures must be considered cautiously because the system is not two-state. Thus, the only rule that can be derived for the effects of the phosphorothioate substitutions on DNA-RNA hybrid duplex stability is that they all appear to be destabilizing. The switch from H15Mg to H12Mg3Mn buffer increases stability for duplexes with and without a single sulfur substitution, and for the isomeric mixture of 5′ exon mimics, d(A*t*T*t*G*t*A*t*C*t*T).

In contrast to phosphorothioates, the phosphoramidate hybrid is 3 kcal/mol more stable than the phosphodiester hybrid (Table 2). This is consistent with previous studies (*19*).

DISCUSSION

Binding enhancement by tertiary interactions (BETI) is a strategy for developing shorter and more specific antisense agents for inhibiting RNA function (*6*, *7*). As illustrated in Figure 4, the free energy increment for binding enhancement by tertiary interactions, $\Delta G°_{BETI}$, is estimated as the difference in free energy for binding a 5′ exon mimic to the P-8/4x ribozyme and to the oligonucleotide r(GGUCAU). The value of $\Delta G°_{BETI}$ is a measure of tertiary stability, i.e., $\Delta G°_{BETI} = RT \ln K_2^{-1}$, where K_2 is the equilibrium constant for formation of tertiary interactions (Figure 4). A goal of this work is to determine if short, chemically stable oligonucleotides are able to exploit tertiary interactions to provide a $\Delta G°_{BETI}$ sufficiently large to give tight and specific binding to an RNA target.

Binding of Phosphorothioate Containing 5′ Exon Mimics. Substitution of individual nonbridging phosphate oxygens with sulfur in the 5′ exon mimic d(ATGACT) does not decrease the tertiary stabilization of the 5′ exon mimic binding to P-8/4x and in some cases increases it (Table 1). The overall strength of binding decreases, however, because of a decrease in the stability of base-pairing of each mimic with the IGS, r(GGUCAU). At every phosphorothioate linkage except for position −3, the S_p isomer binds to P-8/4x less tightly than the R_p isomer. Apparently, the destabilization effects of phosphorothioate substitutions are dependent on the isomer and the position. Therefore, prediction of the destabilizing effects for phosphorothioate substitutions is complex.

The isomeric mixture of 5′ exon mimics with all-phosphorothioate linkages binds to the P-8/4x ribozyme with an apparent K_d greater than 1 μM. This binding is at least 14-fold weaker than d(ATGACT), and is probably too weak to permit effective inhibition of function.

Binding of a Phosphoramidate Containing 5′ Exon Mimic. DNA oligonucleotides with phosphoramidate backbones form stable hybrid duplexes with RNA (*19*, *20*, *32*), and are relatively stable to degradation *in vitro* and *in vivo* (*19*, *33*−*35*). The results in Table 1 show that the phosphoramidate 5′ exon mimic, d(AnTnGnAnCn)rU, binds to the P-8/4x ribozyme almost 4-fold more tightly than d(ATGAC)rU, even though the phosphoramidate mimic shows a 30-fold reduction in tertiary stability. The decrease in tertiary interactions is more than compensated by an increase in the stability of base-pairing. Nevertheless, these results show that phosphoramidate backbones can be used in an antisense strategy based on binding enhanced by tertiary interactions.

Implications for Group I Intron Structure. We have previously shown that the 2′ OH groups of the 5′ exon mimic r(AUGACU) are not required for strong tertiary interactions between the mimic and the catalytic core of the P-8/4x ribozyme (*7*). Here we report that the 10 internal nonbridging phosphate oxygens of the 5′ exon mimic d(ATGACT) can be individually replaced with sulfur (Figure 2) without disrupting the tertiary interactions holding the exon mimic into the catalytic core. This suggests that there are no critical tertiary interactions that require both nonbridging oxygens of a given phosphodiester of the 5′ exon. Furthermore, these substitutions do not change the global helix geometry of the P1 helix such that the helix is prohibited from exploiting other stabilizing tertiary interactions.

Replacing all the internal 3′ O groups of the 5′ exon mimic with NH (Figure 2) decreases the free energy of tertiary interactions by 2 kcal/mol, which is approximately the

Table 1: Thermodynamic Parameters for Binding to P-8/4x and r(GGUCAU) in H15Mg and H12Mg3Mn Buffers[a]

	binding to P-8/4x		binding to r(GGUCAU)		tertiary stability	
oligonucleotide	$K_{d,total}$ (nM)[b]	$-\Delta G°_{37,total}$ (kcal/mol)[c]	$K_{d,BP}$ (mM)[c]	$-\Delta G°_{37,BP}$ (kcal/mol)	$-\Delta\Delta G°_{37,BETI}$ (kcal/mol)[d]	K_2[e]
d(ATGACT)[f]	105.3 ± 43	9.90 ± 0.32	3.35	3.51	6.39	31800
d(AUGACU)[f]	200 ± 111	9.50 ± 0.50	3.46	3.49	6.01	17300
r(AUGACU)[f]	5.21 ± 1.4 (13.9 ± 2.6)[h]	11.75 ± 0.19	0.32	4.96	6.79	61000
d(A*r*TGACT)	289 ± 93 (347)[h]	9.27 ± 0.24	10.11	2.83	6.44	34900
d(A*s*TGACT)	572 ± 188 (1280)[h]	8.85 ± 0.25	19.04	2.44	6.41	33200
d(AT*r*GACT)	301 ± 99	9.25 ± 0.25	8.19	2.96	6.29	27100
d(AT*s*GACT)	415 ± 80	9.05 ± 0.13	18.43	2.46	6.59	44400
d(ATG*r*ACT)	362 ± 69	9.14 ± 0.13	9.47	2.87	6.27	26100
d(ATG*s*ACT)	234 ± 34	9.40 ± 0.10	28.80	2.19	7.22	123100
d(ATGA*r*CT)	185 ± 27	9.55 ± 0.10	25.30	2.27	7.28	136200
d(ATGA*s*CT)	302 ± 67	9.25 ± 0.15	17.99	2.48	6.77	59500
d(ATGAC*r*T)	203 ± 96	9.49 ± 0.39	28.11	2.20	7.29	138500
d(ATGAC*s*T)	600 ± 29	8.83 ± 0.03	32.01	2.12	6.71	53400
d(A*t*T*t*G*t*A*t*C*t*T)	[≥1464 ± 260][i]	≤8.28 ± 0.12	≥6.01	≤3.15	5.13	≈4100
d(ATGACT)[g]	9	11.40	1.70	3.93	7.47	184200
d(ATG*r*ACT)[g]	18	10.99	3.88	3.42	7.57	216700
d(A*t*T*t*G*t*A*t*C*t*T)[g]	65	10.19	1.42	4.04	6.15	21800
d(ATGAC)rU[f]	61.1 ± 7	10.23 ± 0.08	4.07	3.39	6.84	66600
d(AnTnGnAnCn)rU	16 ± 1	11.06 ± 0.04	0.34	6.34	4.72	2130

[a] H15Mg buffer consists of 50 mM Hepes (25 mM Na^+), 15 mM $MgCl_2$, and 135 mM KCl at pH 7.5. H12Mg3Mn is the same as H15Mg except it contains 12 mM $MgCl_2$ and 3 mM $MnCl_2$. All measurements in H15Mg buffer, unless otherwise noted. n represents an N3′→P5′ phosphoramidate linkage. *t* represents a mixture of R_p (*r*) and S_p (*s*) phosphorothioate linkages. Due to potential self-association of r(GGUCAU), $\Delta G°_{37}$ for hybrid duplex formation by sequences with at least one phosphorothioate may be less favorable than indicated (see Materials and Methods). [b] The error is the standard deviation of the measurements for K_d. [c] Calculated from $\Delta G°_{37} = RT \ln(K_d)$ where $R = 0.001987$ kcal mol^{-1} K^{-1} and $T = 310$ K, using more significant digits than listed in this table. [d] Free energy increment from tertiary interactions calculated from the difference in $\Delta G°_{37}$ values for binding to P-8/4x and to r(GGUCAU). [e] Calculated by dividing the K_d value for binding to r(GGUCAU) by the K_d for binding to P-8/4x. The K_2 value was calculated using K_d values containing more significant digits than those listed in this table. [f] See (*7*) for comprehensive thermodynamic analysis. [g] Measured in H12Mg3Mn buffer. [h] Measured by direct band-shift gel electrophoresis. [i] Due to relatively weak binding, the K_d could not be quantified via direct band-shift gel electrophoresis, so the reported value is a lower limit.

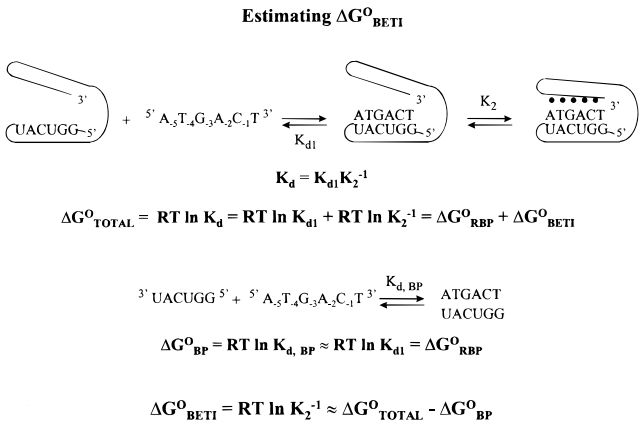

FIGURE 4: Estimating the binding enhancement by tertiary interactions, $\Delta G°_{BETI}$, of a 5′ exon mimic, d(ATGACT), with the P-8/4x ribozyme. K_{d1} is the dissociation constant for the 5′ exon mimic base-pairing to the P-8/4x ribozyme and is assumed to be equivalent to $K_{d,BP}$, which is the dissociation constant for a duplex formed by the hexamers d(ATGACT) and r(GGUCAU).

equivalent of 2 hydrogen bonds (*36*, *37*). The decrease in tertiary stability could result from disrupting specific tertiary interactions between the 5′ exon mimic and the P-8/4x ribozyme. Alternatively, the decrease in tertiary stability could result from a more global helix structure modification that disrupts tertiary interactions between some functional group(s) on the helix formed and the ribozyme.

At this point, tertiary interactions between the 5′ exon mimic and the P-8/4x ribozyme's catalytic core are not known. It is clear, however, that these tertiary interactions must utilize functional groups on the helix other than the 5′ exon mimic's 2′ OH groups (*7*) and internal 3′ oxygens. One possibility is that most of the tertiary contacts form between the catalytic core and the IGS, but only after the IGS base-pairs with the 5′ exon, thus preorganizing various functional groups for tertiary interactions (Figure 1). In support of this, the *Tetrahymena* L-21 *Sca*I ribozyme appears to form more stabilizing tertiary contacts with the IGS than with the 5′ exon (*38*, *39*).

The functional group requirements of the ribozyme for the 5′ exon mimic are surprisingly lax. The ribozyme has the ability to tightly bind 5′ exon mimics that have multiple modifications from its natural substrate. Furthermore, modified 5′ exon mimics with a 3′ terminal rU are substrates for the ribozyme-catalyzed exon-ligation reaction (unpublished experiments), suggesting the functional group requirements for catalytic activity are also lax. This low level of discrimination is highly advantageous for the development of antisense compounds because it allows for modifications that render the antisense nuclease stable without significantly disrupting its binding to the target.

Implications for Antisense Development. We have previously characterized a novel strategy [binding enhanced by tertiary interactions (BETI)] for targeting functionally important RNAs for pharmacological intervention (*7*). This strategy takes advantage of the enhanced binding and specificity that occurs when short oligonucleotides exploit

Table 2: Thermodynamic Parameters for Binding to r(GGUCAU) in H15Mg and H12Mg3Mn Buffers[a]

	$1/T_M$ vs $\log(C_T/4)$ parameters				curve fit parameters			
oligonucleotide	$-\Delta G°_{37}$ (kcal/mol)[b]	$-\Delta H°$ (kcal/mol)[b]	$-\Delta S°$ (eu)[b]	T_M (°C)[c]	$-\Delta G°_{37}$ (kcal/mol)[b]	$-\Delta H°$ (kcal/mol)[b]	$-\Delta S°$ (eu)[b]	T_M (°C)[c]
d(ATGACT)[e]	3.51 ± 0.03	55.07 ± 0.6	166.27 ± 2.1	20.9	3.77 ± 0.11	49.82 ± 2.2	148.45 ± 7.4	20.7
d(A*r*TGACT)					2.83	51.09	155.61	18.2
d(A*s*TGACT)					2.44	53.65	165.09	17.0
d(AT*r*GACT)					2.96	47.99	145.21	17.6
d(AT*s*GACT)					2.46	51.19	157.13	16.5
d(ATG*r*ACT)					2.87	54.31	165.85	18.4
d(ATG*s*ACT)					2.19	46.21	141.93	12.9
d(ATGA*r*CT)					2.27	54.09	167.10	16.5
d(ATGA*s*CT)					2.48	55.66	171.45	17.7
d(ATGAC*r*T)					2.20	56.29	174.40	17.0
d(ATGAC*s*T)					2.12	51.62	159.59	15.0
d(A*t*T*t*G*t*A*t*C*t*T)	3.15 ± 0.10	57.64 ± 1.7	175.69 ± 5.9	19.8	3.06 ± 0.36	57.85 ± 6.5	176.69 ± 22	19.4
d(ATGACT)[d]					3.93	51.87	154.56	15.8
d(ATG*r*ACT)[d]					3.42	54.31	164.10	14.2
d(A*t*T*t*G*t*A*t*C*t*T)[d]					4.04	58.32	175.02	17.6
d(ATGAC)rU[e]	3.39 ± 0.16	56.73 ± 2.8	171.97 ± 9.4	20.7	3.51 ± 0.27	52.98 ± 6	159.49 ± 20	20.3
d(AnTnGnAnCn)rU	6.34 ± 0.01	39.47 ± 0.5	106.80 ± 1.7	35.5	6.36 ± 0.21	46.77 ± 3.8	130.27 ± 12	35.9

[a] H15Mg buffer consists of 50 mM Hepes (25 mM Na^+), 15 mM $MgCl_2$, and 135 mM KCl at pH 7.5. H12Mg3Mn is the same as H15Mg except it contains 12 mM $MgCl_2$ and 3 mM $MnCl_2$. All measurements in H15Mg buffer, unless otherwise noted. n represents an N3′→P5′ phosphoramidate linkage. *t* represents a mixture of R_p (*r*) and S_p (*s*) phosphorothioate linkages. Due to potential self-association of r(GGUCAU), $\Delta G°_{37}$ for hybrid formation by sequences with at least one phosphorothioate may be less favorable than indicated (see Materials and Methods). [b] The errors are based on the standard deviations of the thermodynamic parameters and were calculated as described (*42*−*44*). Considering all sources of error for T_m^{-1} vs $\log(C_T/4)$ parameters, the typical error estimate for $\Delta G°_{37}$ is 4%, $\Delta H°_{37}$ is 12%, and $\Delta S°_{37}$ is 13.5%. Significant figures are given beyond error estimates to allow accurate calculation of T_m and other parameters. [c] Calculated for 10^{-4} M oligonucleotide concentration. [d] Measured in H12Mg3Mn buffer. [e] From (*7*).

stabilizing tertiary interactions with RNA targets (see Figure 1). The results in Table 1 show that certain modifications that protect against cellular nucleases do not eliminate the hexanucleotide's ability to exploit tertiary interactions for binding the ribozyme's catalytic core.

DNA 5′ exon mimics that contain a single R_p or S_p phosphorothioate linkage have reduced base-pairing stability with the RNA IGS mimic, GGUCAU, as expected (*40*), but do not reduce, and in some cases enhance, tertiary stabilization. This effectively increases the specificity of tertiary-site targeted antisense oligonucleotides because the low stability of base-pairing reduces the possibility of antisense oligonucleotides base-pairing to their complements in other RNA contexts. Unfortunately, hexanucleotides with all-phosphorothioate linkages bind to the ribozyme weakly. These results suggest that antisense oligonucleotides partially substituted with phosphorothioate linkages might be more effective for BETI than those completely substituted. It has been suggested that DNA oligonucleotides with all-phosphorothioate linkages might cause nonspecific inhibitory effects *in vivo* (*11*, *12*). If true, then limiting the number of phosphorothioate linkages might reduce these nonspecific effects (*41*) and perhaps could be as effective at preventing nuclease degradation (*9*).

In contrast to the 5′ exon mimics with multiple phosphorothioate linkages, the 5′ exon mimic with N3′→P5′ phosphoramidate linkages at every internal position bind to the ribozyme's catalytic core more tightly than the unmodified mimic. Therefore, antisense oligonucleotides with N3′→P5′ phosphoramidate linkages might be more effective than those with phosphorothioate linkages. Furthermore, N3′→P5′ phosphoramidates are nonchiral, which greatly simplifies the purification and analysis of these compounds compared to phosphorothioates.

These results demonstrate that 5′ exon mimics of the group I intron from the opportunistic pathogen *P. carinii* can be chemically modified for nuclease stability without eliminating the tertiary interactions that are required for binding of the mimic *in vitro* to the catalytic core of the ribozyme. Preliminary results indicate the phosphoramidates are also active substrates when bound to a *P. carinii* group I intron precursor, so that it may be possible to use such compounds as suicide inhibitors of splicing (unpublished experiments).

ACKNOWLEDGMENT

The authors thank an anonymous reviewer for helpful comments on the manuscript, Thomas W. Barnes III for mass spectroscopic analysis of d(AnTnGnAnCn)rU, and Tianbing Xia for discussions on error estimates.

REFERENCES

1. Sogin, M. L., and Edman, J. C. (1989) *Nucleic Acids Res. 17*, 5349−5359.
2. Liu, Y., Rocourt, M., Pan, S., Liu, C., and Leibowitz, M. J. (1992) *Nucleic Acids Res. 20*, 3763−3772.
3. Mei, H.-Y., Cui, M., Suttons, S. T., Truong, H. N., Chung, F.-Z., and Czarnik, A. W. (1996) *Nucleic Acids Res. 24*, 5051−5053.
4. Chrissey, L. (1991) *Antisense Res. Dev. 1*, 65−113.
5. Baserga. R., and Denhardt, D. T., Ed. (1992) *Antisense Strategies*; Annals of the New York Academy of Sciences 660; New York Academy of Sciences: New York.
6. Bevilacqua, P. C., and Turner, D. H. (1991) *Biochemistry 30*, 10632−10640.
7. Testa, S. M., Haidaris, C. G., Gigliotti, F., and Turner, D. H. (1997) *Biochemistry 36*, 15303−15314.
8. Wickstrom, E. (1986) *J. Biochem. Biophys. Methods 13*, 97−102.

9. Shaw, J.-P., Kent, K., Bind, J., Fishback, J., and Froehler, B. (1991) *Nucleic Acids Res. 19*, 747−750.
10. Uhlmann, E., and Peyman, A. (1990) *Chemical Reviews 90*, 543−584.
11. Milligan, J. F., Matteucci, M. D., and Martin, J. C. (1993) *J. Med. Chem. 36*, 1923−1937.
12. Matteucci, M. D., and Wagner, R. W. (1996) *Nature 384*, 20−22.
13. Rawls, R. (1997) *Chem. Eng. News 75*, 35−39.
14. Freier, S. M., and Altmann, K.-H. (1997) *Nucleic Acids Res. 25*, 4429−4443.
15. Eckstein, F. (1979) *Acc. Chem. Res. 12*, 204−210.
16. Stec, W. J., Zon, G., Egan, W., and Stec, B. (1984) *J. Am. Chem. Soc. 106*, 6077−6079.
17. Eckstein, F. (1985) *Annu. Rev. Biochem. 54*, 267−402.
18. Gryaznov, S. M., and Letsinger, R. L. (1992) *Nucleic Acids Res. 20*, 3403−3409.
19. Gryaznov, S. M., and Chen, J.-K. (1994) *J. Am. Chem. Soc. 116*, 3143−3144.
20. Gryaznov, S. M., Lloyd, D. H., Chen, J.-K., Schultz, R. G., DeDionisio, L. A., Ratmeyer, L., and Wilson, W. D. (1995) *Proc. Natl. Acad. Sci. U.S.A. 23*, 1292−1299.
21. Iyer, R. P., Egan, W., Regan, J. B., and Beaucage, S. L. (1990) *J. Am. Chem. Soc. 112*, 1253−1254.
22. Wilk, A., and Stec, W. J. (1995) *Nucleic Acids Res. 23*, 530−534.
23. Potter, B. V. L., Connolly, B. A., and Eckstein, F. (1983) *Biochemistry 22*, 1369−1377.
24. Puglisi, J. D., and Tinoco, I., Jr. (1989) *Methods in Enzymology 180*, 304−325.
25. Longfellow, C. E., Kierzek, R., and Turner, D. H. (1990) Biochemistry *29*, 278−285.
26. McDowell, J. A., and Turner, D. H. (1996) *Biochemistry 35*, 14077−14089.
27. Borer, P. N., Dengler, B., Tinoco, I., Jr., and Uhlenbeck, O. C. (1974) *J. Mol. Biol. 86*, 843−853.
28. Dahm, S. C., and Uhlenbeck, O. C. (1991) *Biochemistry 30*, 9464−9469.
29. Christian, E. L., and Yarus, M. (1993) *Biochemistry 32*, 4475−4480.
30. Piccirilli, J. A., Vyle, J. S., Caruthers, M. H., and Cech, T. R. (1993) *Nature 361*, 85−88.
31. Kibler-Herzog, L., Zon, G., Uznanski, B., Whittier, G., and Wilson, W. D. (1991) *Nucleic Acids, Res. 19*, 2979−2986.
32. Ding, D., Gryaznov, S. M., Lloyd, D. H., Chandrasekaran, S., Yao, S., Ratmeyer, L., Pan, Y., and Wilson, W. D. (1996) *Nucleic Acids Res. 24*, 354−360.
33. Gryaznov, S. M., Skorski, T., Cucco, C., Nieborowska-Skorska, M., Chiu, C. Y., Lloyd, D., Chen, J.-K., Koziolkiewicz, M., and Calabretta, B. (1996) *Nucleic Acids Res. 24*, 1508−1514.
34. Escudé, C., Giovannangeli, C., Sun, J.-S., Lloyd, D. H., Chen, J.-K., Gryaznov, S. M., Garestier, T., and Hélène, C. (1996) *Proc. Natl. Acad. Sci. U. S.A. 93*, 4365−4369.
35. Skorski, T., Perotti, D., Nieborowska-Skorski, M., Gryaznov, S. M., and Calabretta, B. (1997) *Proc. Natl. Acad. Sci. U.S.A. 94*, 3966−3971.
36. Turner, D. H., Sugimoto, N., Kierzek, R., and Dreiker, S. D. (1987) *J. Am. Chem. Soc. 109*, 3783−3785.
37. SantaLucia, J., Jr., Kierzek, R., and Turner, D. H. (1992) *Science 256*, 217−219.
38. Strobel, S. A., and Cech, T. R. (1993) *Biochemistry 32*, 13593−13604.
39. Strobel, S. A., and Cech, T. R. (1995) *Science 267*, 675−679.
40. Stein, C. A., Subasinghe, C., Shinozuka, K., and Cohen, J. S. (1988) *Nucleic Acids Res. 16*, 3209−3221.
41. Agrawal, S., and Akhtar, S. (1995) *Trends Biotech. 13*, 197−199.
42. SantaLucia, J. Jr., Kierzek, R., and Turner, D. H. (1991a) *J. Am. Chem. Soc. 113*, 4313−4322.
43. SantaLucia, J. Jr., Kierzek, R., and Turner, D. H. (1991b) *Biochemistry 30*, 8242−8251.
44. Xia, T., McDowell, J. A., and Turner, D. H. (1997) *Biochemistry 36*, 12485−12497.
45. Michel, F., and Westhof, E. (1990) *J. Mol. Biol. 216*, 585−610.

BI980092T